Impact of climate change on surface runoff: a case study of the Darabad River, northeast of Iran

Hamid Reza Zakizadeh, Hassan Ahmadi, Gholam Reza Zehtabiyan, Abolfazl Moeini and Alireza Moghaddamnia

ABSTRACT

Climate change is one of the major challenges affecting natural ecosystems and various aspects of human life. The effects of global warming on the hydrology and water cycle in nature are very serious, and the quantitative recognition of these effects creates more readiness to deal with its consequences. In the present study, the 2006–2100 period is predicted based on the statistical downscaling model (SDSM). Finally, the effects of climate change on the hydrological conditions in the Darabad watershed are simulated using the soil and water assessment tool (SWAT) model. The SWAT model calibration is done based on the SUFI-2 algorithm, and the effective and optimal parameter is identified. The results of the study, while confirming the efficiency of both SDSM in climate simulations and SWAT in hydrological simulation, showed that the increase in precipitation and temperature is probably in future climate conditions for the 2010–2040 period. The surface flow and runoff at the watershed area during the observation period (1970–2010) is 0.29 m^3/s, but this value for the predicted period with regard to climate change in the RCP 2.6, RCP 4.5, and RCP 8.5 scenarios is equal to 0.43, 0.44, and 0.45 m^3/s. The results of research, while highlighting the importance of effects of climate change, make it essential to apply them for proper management in order to adapt to climate change in the future policies of the Darabad watershed management.

Key words | CanESM2, climate change, RCP, SDSM, SWAT

Hamid Reza Zakizadeh
Hassan Ahmadi (corresponding author)
Abolfazl Moeini
Department of Forest, Range and Watershed Management, Science and Research Branch,
Islamic Azad University,
Tehran,
Iran
E-mail: *ahmadi@ut.ac.ir*

Gholam Reza Zehtabiyan
Alireza Moghaddamnia
Department of Reclamation of Arid and Mountainous Regions,
University of Tehran,
Karaj,
Iran

HIGHLIGHTS

- Evaluation of climate change effects on surface runoff.
- SWAT model, the best simulation daily runoff for watershed.
- The model predicted average temperature increase by 2006–2100 of 6 °C by the CanEMS2.
- Precipitation in the upcoming period of 2006–2100 shows a 52% increase.
- The runoff in the upcoming periods of 2006–2040 under RCP 2.6, RCP 4.5, and RCP 8.5 scenarios is increased by 45, 49, and 50%, respectively.

INTRODUCTION

Today, numerous studies have been conducted in Iran and around the world regarding the potential impacts of climate change on water resources, including the impact on water quantity, hydrology, and water demand. Using global data available from the last century, it was found that the global runoff is increased by 4% with the earth temperature rising by 1% (Vera *et al.* 2006; Narsimlu *et al.* 2013).

The increase in temperature, severe droughts, rise in sea levels, exacerbation of climate phenomena, the melt of mountain glaciers, and decrease in polar ice glaciers are among the

doi: 10.2166/wcc.2020.089

effects of climate change. Climate change leads to dramatic changes in hydrosphere, biosphere, and ecosphere, with hydrological consequences such as water stresses.

Water stresses are caused by a set of factors, such as rising temperatures, droughts, and changes in water consumption pattern (Raziei *et al.* 2005). Meanwhile, the temperature has a greater role in creating water stress than the other climate elements due to its effects on the hydrological cycle (precipitation, evapotranspiration, and interception) (Huo & Li 2013). Therefore, with the continuation of global climate change and its impact on water resources, it is expected to affect more than 4 billion inhabitants of the earth. In fact, the climate of the planet is changing, and global warming is taking place (Narsimlu *et al.* 2013; Klein 2015).

The consequences of this change include the changes in climate elements, especially temperature and precipitation in different regions. This phenomenon occurs due to the increase in the concentration of greenhouse gases in the atmosphere (Sanz-Perez *et al.* 2016).

According to the report, over the last century, the average annual temperature of the planet has increased 0.3–0.6 °C due to greenhouse gas emissions and is expected to increase about 1–3.5 °C by 2100 (Houghton *et al.* 1991).

The process of climate change, especially temperature and precipitation changes, is the most important issue in the field of environmental sciences. This phenomenon is of increasing importance due to its scientific and applied dimensions (environmental and socioeconomic effects), as human systems dependent on the climate elements such as agriculture, industry and the like are designed based on the stability and sustainability of the climate (Huo & Li 2013).

Climate change creating drought phenomena and the impact on its intensity and continuity reduces vegetation, and consequently, influences on the hydrological responses in the watershed area (Tavakol-Davani *et al.* 2013).

Also, the increase in air temperature due to climate change will change the precipitation from snow to rain, and change the amount and intensity of runoff, ratio of snow to rain, and amount of water stored in the snow mass. As a result, the amount of precipitation as snow in the middle and low heights of mountainous regions is reduced and increased in the highlands, which ultimately affects the peak daily flow rate (Rahimi *et al.* 2018).

The Intergovernmental Panel on Climate Change (IPCC) suggests that in recent decades, climate change has globally changed the hydrological characteristics, so that precipitation and surface flow are higher in the upper and middle latitudes and are lower in the lower latitudes, and the probability of confrontation with extreme climatic events such as floods and droughts will be increased (Narsimlu *et al.* 2013).

In order to investigate the effects of climate change on different systems in upcoming periods, the future climate variables should be initially simulated. There are several methods for simulating climate variables in the upcoming periods, and the most valid method is the use of climate outputs of atmosphere–ocean general circulation models (AOGCM). In these models, efforts have been made to simulate the processes that are effective on the climate and the climate situation to be predicted for the upcoming years based on the processes. Since the prediction of future climate conditions is not possible under the influence of the climate change phenomenon, the alternative solution is to determine the possibility of various events, which is ultimately performed using the emission scenarios (Ashraf Vaghefi *et al.* 2014; Dehghan *et al.* 2019).

One of the drawbacks of large-scale models is the large size of the computational cell, which should be localized and scaled down using the downscaling method. In this research, the statistical downscaling model (SDSM) was used for the downscaling. One of the reasons for choosing the SDSM is the proper performance for the downscaling in Iran (Tavakol-Davani *et al.* 2013; Zehtabian *et al.* 2016) and outside Iran (Gagnon *et al.* 2005; Hassan *et al.* 2014).

Many models have been proposed to study global climate change and its impact on hydro-geomorphological characteristics of the watershed. However, in this research, the selection, calibration, and simulation of the watershed were done given the capabilities of the SDSM for climate prediction and also, according to the wide and successful application of the soil and water assessment tool (SWAT) model in Iran and the world for the hydrological simulation.

In general, various studies have been conducted on the SWAT model which evaluated its performance in the simulation of precipitation-runoff (Al-mukhtar 2016; Gyamfi *et al.* 2016; Dhami *et al.* 2018).

Awan *et al.* (2016) studied the effects of climate change on runoff in India under two RCP 4.5 and RCP 8.5 scenarios. The main focus of the research was generally on the evaluation of the performance of the SWAT model. In this research, the SWAT model has a Nash–Sutcliffe efficiency (NSE) coefficient of 0.83. The results of this study showed that in the upcoming period, the accessible water levels would be increased by 7–11% in the mentioned scenarios.

da Silva *et al.* (2018) evaluated the performance of the SWAT model in Cerrado biome. The research was done in three watersheds. In general, the NSE coefficient was 0.8, 0.76, and 0.6, respectively.

Shahvari *et al.* (2019) evaluated the effect of climate change on evapotranspiration in the Varamin plain. In this research, the climate change results were obtained based on three scenarios from the fifth-generation report, and the SWAT model was also used. The results of this study showed that the highest increase in all three scenarios is related to RCP 8.5 in the period of 2070–2100.

Jaiswal *et al.* (2017) studied the effects of climate change in India under three RCP 2.6, RCP 4.5 and RCP 8.5 scenarios. The results of this study showed that the precipitation was decreased by about 12–29% in the range 2020–2099.

Nazari-Sharabian *et al.* (2019) evaluated the impact of climate change in Iran. In general, the stormwater management model was used in this research. The results of this study showed that the amount of runoff in the upcoming period rises by 23–27%.

Dinpashoh *et al.* (2019) evaluated the effects of climate change in Iran. The results of this study showed that during the upcoming period, the amount of precipitation is decreased and instead, the intensity of precipitation in the upcoming period, and finally, the average monthly precipitation shows an increasing trend.

In general, by studying the effects of climate change, we conclude that the climate change performance on the runoff greatly varies, so that some cases show the precipitation and runoff decreases and some others show the precipitation and runoff increases. However, in all reports, there is an evident increase in temperature in the upcoming period. In general, in this research, the study area is located upstream of the Tehran watershed, and the study of climate and its effects on runoff are very important. This is especially manifested when there is a large population downstream of the watershed. In fact, flood and drought are more likely to happen in these situations.

Generally, the objectives of the research are as follows:

(1) evaluation of the performance of CanEMS2 climate change model and SDSM,
(2) evaluation of the performance of the SWAT model in the precipitation-runoff simulation,
(3) evaluation of precipitation and runoff variations in upcoming period (2006–2100), and
(4) study of runoff variations in upcoming period (2010–2040).

MATERIALS AND METHODS

Study area

Darabad watershed (Figure 1) with a total area of 1,727 hectares is located in the county of Shemiranat. Geography 51° 35′ to 51° 45′ east and 35° 81 to 35° 87′ northern latitude, which is limited to the village of Roodbar Ghasran from the north, and to one of the municipalities of Tehran from the south, and to the valley of Yurt Cheshmeh, and to Golab Darreh and Darband from the west.

The highest point of the area has a height of 3,539 m, and the lowest elevation is at its output 1,704 m above sea level. Rainfall in Darabad River watershed mainly occurs in the autumn and winter, and the average annual precipitation of this area is about 790 mm. The mean maximum temperature in this area is about 12.75 °C, and the mean minimum is about 2.37 °C.

Datasets and input data

To simulate rainfall–runoff and climate change in this study, we need daily time series of climate data and maps. Daily data include rainfall, maximum temperature, minimum temperature, relative humidity, wind speed, flow rate, and amount of sunlight. Table 1 and Figure 1 show the features of the stations used. In order to check and control the input data into the precipitation-runoff model in terms of accuracy, precision, and adequacy, we began by forming the time series of the precipitation data, maximum and minimum

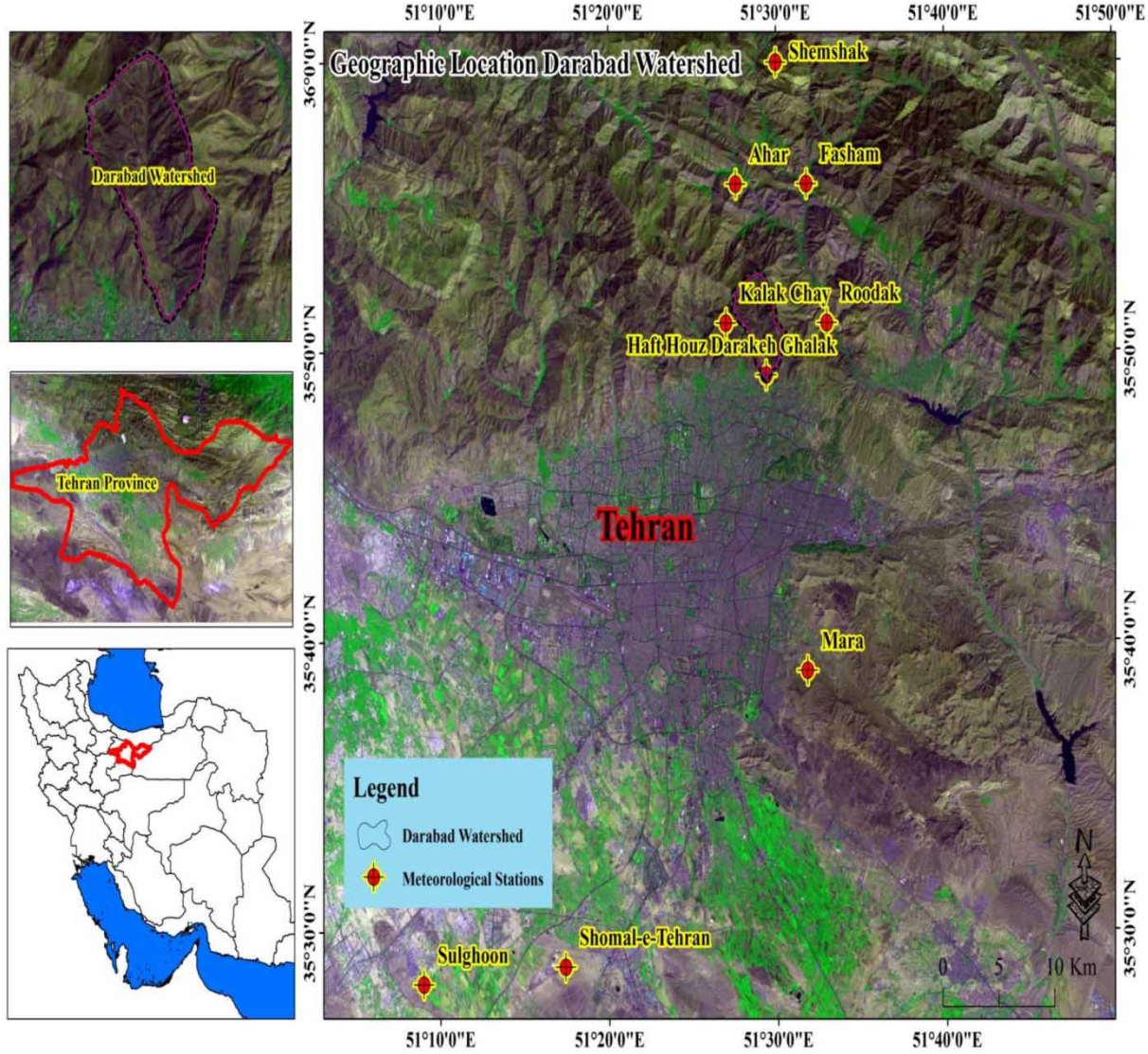

Figure 1 | Location of the Darabad watershed in Iran.

temperatures, wind speed, and relative humidity and then correcting and reconstructing the data gaps and outliers using the methodology proposed by the American Water Resources Association (AWRA) (Ahmadi *et al.* 2019a, 2019b).

Using the AWRA-proposed methodology, the mean, upper bound, lower bound, and standard deviation of the data were evaluated. The coefficient of determination of the outliers was calculated using the tables provided by the AWRA at a significance level of 10% considering normal distribution.

The so-called run-test was performed to investigate the homogeneity of the time series data. For this purpose, the data points were sorted in ascending or descending order. Then, the median was identified, and the state of each data point with respect to the median (larger or smaller than the median) was signified by a particular sign. Finally, the upper and lower bounds of the existing ranges are calculated using the related table (Ahmadi *et al.* 2019a, 2019b).

To prepare the precipitation-runoff model, it is necessary to use validated data. Any error in the input data of the model can be an important factor in the error in the estimated model and simulated flow parameters.

The required meteorological data are precipitation, minimum and maximum daily temperature, radiation,

Table 1 | Weather stations with geographical coordinates located in Darabad watershed

The length of the statistical period	Station type	Meters above sea level	Latitude	Longitude	River	Station name
1973–2010	Hydrometery	1706	51.49	35.82	Darabad	Ghalak
1990–2010	Hydrometery	1700	51.49	35.82	Darakeh	Haft Houz Darakeh
1970–2010	Hydrometery	1430	51.15	35.47	Kan	Sulghoon
1961–2010	Synoptic	1190	51.19	35.41	–	Mehr Abad
1987–2010	Synoptic	1549	51.29	35.48	–	Shomal-e-Tehran
1971–2010	Rain gauge	2100	51.46	35.93	Jajrood	Ahar
1973–2010	Rain gauge	1940	51.53	35.93	Ab Migoon	Fasham
1975–2010	Rain gauge	2700	51.5	36	Jajrood	Shemshak
1968–2010	Rain gauge	1710	51.55	35.85	Jajrood	Roodak
1990–2010	Rain gauge	2470	51.45	35.85	–	Kalak Chay
1982–2010	Rain gauge	1810	51.53	35.65	–	Mara

wind speed, and relative humidity. In addition to the above, the maps including topography, weather, vegetation, soil and management data, and topographic data in the form of digital elevation model (DEM) (Figure 2) should be entered into the model as a raster and specific geographic coordinate system. Taking into account the digital elevation, the model is able to determine the location of river streams and watersheds of each one with the desired accuracy. Thus, by entering a value (desired minimum area), the region is divided into smaller sub-basins. The land use and soil map of 1:250,000 scale was obtained, and the land use map was extracted from the satellite images. Also, in this research, a DEM with the 30 m accuracy was used.

After collecting the raw data and preparing the input files, the model implementation steps are as follows:

(1) Enter the DEM and determine watershed sub-basins and physical characteristics such as area and length of main streams,
(2) Enter land use map, soil and slope information and generate hydrological response units based on desired information,
(3) Introduce meteorological data on a daily basis,
(4) Extract hydrological parameters,
(5) Calibrate the SWAT model based on SUFI-2 algorithm, and
(6) Simulate runoff for period 2010–2040.

The table below shows the location of the used stations.

Emission scenario and downscaling

The process of climate change, especially temperature and precipitation changes, is the most important issue in the field of environmental sciences. At present, the most valid tool for producing climate scenarios is the 3D coupled AOGCM. In this study, the CanESM2 model is used which incorporates three representative concentration pathway (RCP) (2.6, 4.5, and 8.5) scenarios in 2006–2100 and NCEP data from 1961 to 2005.

The emission scenarios are used to predict the concentration of greenhouse gases in the atmosphere. The IPCC used the RCP scenario as representatives of various trajectories of greenhouse gas concentrations for compiling the fifth report. In this study, the RCP (2.6, 4.5, and 8.5) scenarios are cited. The RCP 8.5 scenario encompasses the highest rate of increased greenhouse gases and the resulting radiative forcing, which will be progressed in this scenario without adopting any climate consequence mitigation and prevention policies, while the RCP 2.5 scenario includes the lowest rate of increased greenhouse gases and radiative forcing (Mirdashtvan *et al.* 2018).

The output of the general circulation model is downscaled by two statistical and dynamic methods (Samadi *et al.* 2013). In this research, the SDSM as a statistical method is used for the downscaling. The SDSM is an auxiliary tool for assessing the effects of local climate change which is developed by Wilby *et al.* (2002). This model uses

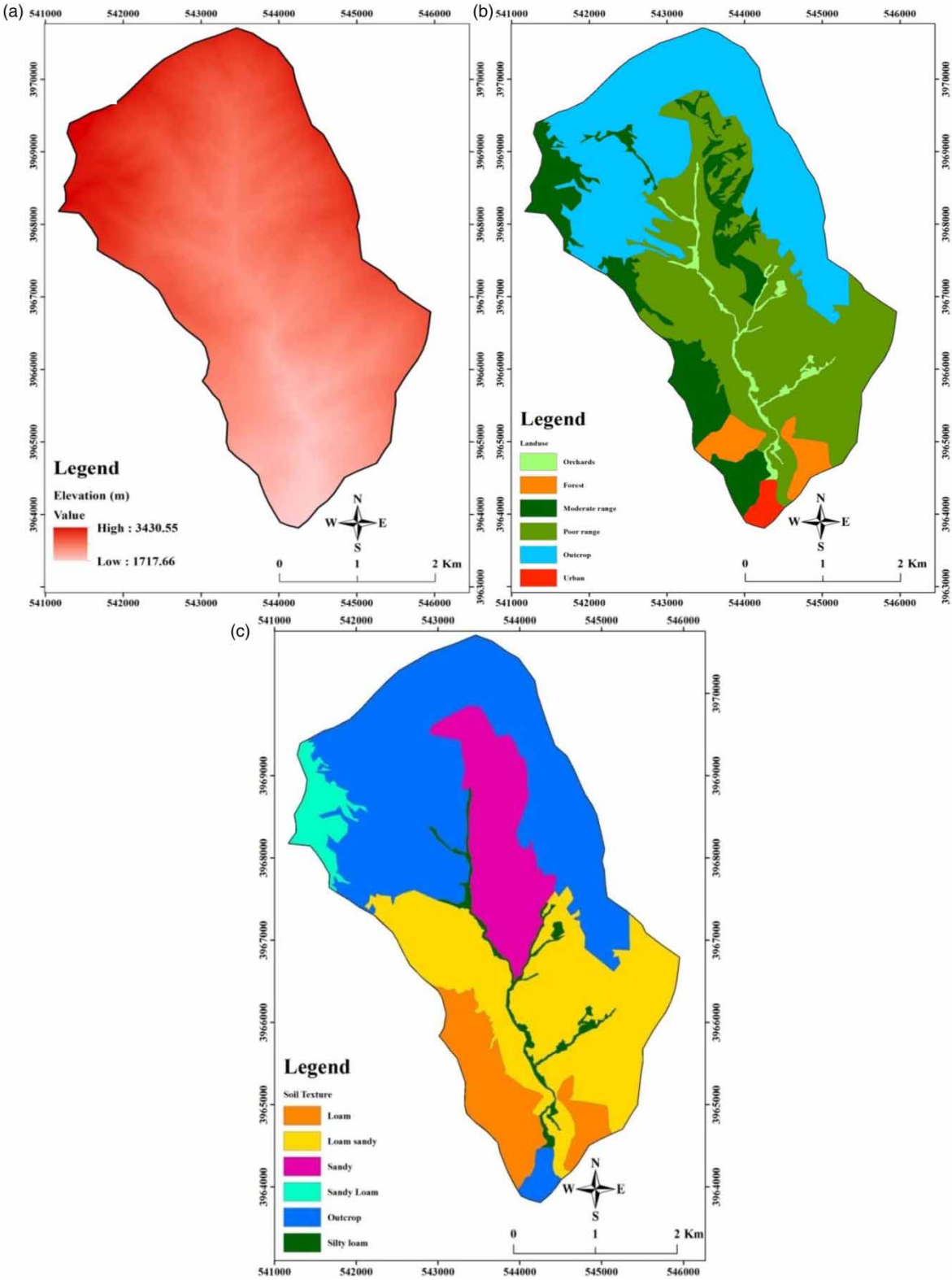

Figure 2 | (a) DEM map, (b) land use map, and (c) soil map.

independent observational data to assess the relationship between local downscaled variables and atmospheric upscaled variables (Wilby & Dawson 2007).

In order to simulate the future-period precipitation and maximum and minimum temperatures, one should use the SDSM to develop multivariate regression equations relating the mentioned variables to the 26 parameters of the NCEP. Table 6 presents a list of the NCEP parameters.

SWAT hydrological model

SWAT is a hydrological, continuous-time, distributed, and physically based model. This model has shown that it has a great deal of accuracy due to numerous projects at the international level (Deng *et al.* 2014; Al-mukhtar 2016). Therefore, instead of using regression relations for the SWAT input and output, there is a need for specific information on the climate, soil properties, topography, and land cover type (Park *et al.* 2014). The physical processes related to the movement of water, sediment, plant growth, food cycle in soil, etc. are among those that are simulated using the mentioned inputs (Gyamfi *et al.* 2016). Among the main advantages of using this model are (1) ability to simulate watersheds without the measurement station and (2) evaluation of response for new inputs (change in management practices of the watershed, land use, etc.).

In this model, watersheds are divided into a number of sub-basins and the sub-basins into the hydrologic response units (HRUs). These units are as similar as possible and have the same combination of soil, topography, and vegetation. This division enables the models to reflect the differences in evaporation and transpiration for different soils and plants. The model uses the modified Green-Ampt curve number to calculate surface runoff. Also, the runoff is separately simulated in each HRU, and one of the Muskingum or variable storage routing methods is used to determine the total watershed runoff. In this way, the simulation accuracy is enhanced and a better physical explanation of the water equilibrium equation is expressed. The Muskingum method was used in this research (Awan *et al.* 2016; Worqlul *et al.* 2018).

The calibration of watershed simulation models has many problems since there are uncertainties in the forms such as simplified processes that are not considered, and the processes in the watershed which are not specified for the modeling (Rostamian *et al.* 2008). The examples of these include the effect of a reservoir on the hydrology of the river transition material, interfering effect between surface and underground waters, effect of constructing structures such as dams and bridges that can have a strong effect on the pattern of flow and sedimentation, unknown flow of sewage discharge into the river, and other issues, including agricultural irrigation management programs. Due to the different uncertainties and distribution of the model, it is important to calibrate this model for the watershed.

In the present study, the SUFI2 model was used for calibration and uncertainty. The SWAT-CUP is a linking optimizer program developed for the SWAT model, which makes it easy to calibrate and analyze the uncertainties of the SWAT model (Arnold *et al.* 2012; Abbaspour *et al.* 2015; Noori & Kalin 2016).

In general, in the previous study, the period of 1980–1988 was used as the calibration period, and the period of 1990–1998 was used for validation. The reason for choosing this period is that both the period of drought and rainy period are in it, it is statistically desirable and required less reconstruction, and it is necessary to note that the SWAT model was executed from 1970 to 2008 and the period of 1970–1972 was used to warm up the model.

Error and uncertainty analysis

In order to determine the reliability of the simulated data, the mean and two statistical indicators, namely NSE (Equation (1)) and coefficient of determination (R^2) (Equation (2)) and mean bias error (MBE) (Equation (3)), are used.

The R^2 value represents a linear relationship between the simulated and observational data, which ranges from zero to one, and the values closer to one represent better simulation. For determining the model efficiency, it was found that if the values of NSE coefficient are more than 0.75, the simulation is good, the values between 0.36–0.75 show a satisfactory simulation, and the values less than 0.36 represent an unacceptable simulation

(Jimeno-Sáez *et al.* 2018).

$$\mathrm{NSE} = 1 - \frac{\sum_{i=1}^{n} (Q_i - S_i)^2}{\sum_{i=1}^{n} (Q_i - \bar{Q})^2} \quad (1)$$

$$R^2 = \frac{\sum_{i=1}^{n} (Q_i - S_i) - (S_i - \bar{S})^2}{\sum_{i=1}^{n} (Q_i - \bar{Q})^2 - \sum_{i=1}^{n} (S_i - \bar{S})^2} \quad (2)$$

$$\mathrm{MBE} = \frac{\sum (Q_i - S_i)^2}{n} \quad (3)$$

Q_i, observed; $\bar{Q}$, mean observed; S_i, simulated; $\bar{s}$, mean simulated; and n, number of data.

Used in the SWAT-CUP, the SUFI-2 algorithm not only calibrated the SWAT model but could also be used to examine possible error and uncertainty. In the present work, monthly data were used to check the calibration and uncertainty of the precipitation-runoff data. Based on the studies performed by Jimeno-Sáez *et al.* (2018), the results are not satisfactory, satisfactory, fairly good, and very good if the value of the NSE is smaller than 0.3, ranges between 0.3 and 0.5, ranges between 0.5 and 0.7, and exceeds 0.7, respectively.

RESULTS

Error and uncertainty analysis of climate model and hydrologic model

Table 2 shows the predictor variables among 26 NCEP variables for the maximum temperature and minimum temperature in the precipitation, maximum temperature, and minimum temperature parameters. As can be seen, total precipitation is a constant variable in the precipitation of the study area and air temperature at 2 m is a constant variable in the temperature of the study area.

To select the appropriate NCEP variables in the SDSM, 70% of the data for training and 30% for the evaluation were selected, but in this research, the historical data were used to evaluate the performance of the SDSM from 1961 to 2005.

In the simulation of the present and future maximum and minimum temperatures, the air temperature 2 m was among the most important parameters contributing to the simulation of the maximum and minimum temperatures.

Table 2 | Variables selected for precipitation, minimum temperature, and maximum temperature of the study area

Station name	T Max Mehrabad	T Min Mehrabad	T Max Shemiranat	T Max Shemiranat	Rain Mehrabd	Rain Shemiranat	Rain Fasham	Rain Roodak	Rain Roodbar Ghasran
Predictor	Air temperature at 2 m	Air temperature at 2 m	Air temperature at 2 m	Air temperature at 2 m	Total precipitation	Total precipitation	Total precipitation	Total precipitation	Total precipitation
	500 hPa Geopotential velocity	Surface meridional velocity	500 hPa Geopotential velocity	Surface meridional velocity	500 hPa Specific humidity	850 hPa Divergence of true wind	850 hPa Divergence of true wind	1,000 hPa Specific humidity	500 hPa Specific humidity
	850 hPa Zonal velocity	500 hPa Airflow strength	Surface meridional velocity	Near surface relative humidity	1,000 hPa Specific humidity	Air temperature at 2 m	500 hPa Divergence	500 hPa Geopotential	Air temperature at 2 m
	Near surface relative humidity	850 hPa Zonal velocity		850 hPa Zonal velocity	500 hPa Meridional wind component	850 hPa Specific humidity	1,000 hPa Divergence of true wind	500 hPa Meridional wind component	500 hPa Geopotential
					1,000 hPa Divergence of true wind				500 hPa Divergence

By examining the error of the SDSM in the CanESM2 scenario for the precipitation parameter (Figure 3(a)), the highest error of the model occurred at the Roodak station and the model had a 12 mm overestimation in the annual results. The lowest error was obtained at Shemiranat and Mehr Abad stations (3 mm decrease and 3 mm increase, respectively). At the Roodbar Ghasran and Fasham stations, the model has 11 and 9 mm increased error in the average annual, respectively. The highest error was reported in Fasham, Roodbar Ghasran, Roodak, Mehr Abad, and Shemiranat stations in February (27 mm), November (30 mm), April (28 mm), November (13 mm),

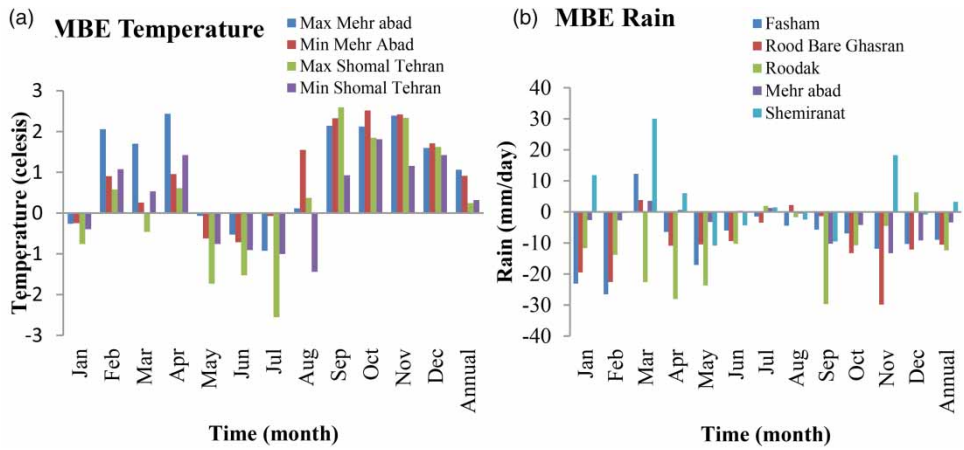

Figure 3 | Review of MBE for (a) precipitation, (b) maximum temperature and minimum temperature parameters.

Table 3 | Features of calibration parameters, minimum values, maximum values, and proportional values

Parameter_Name	Description	Fitted_Value	Min_Value	Max_Value
1:V__GW_REVAP.gw	Groundwater REVAP coefficient	213,426,432.00	−256,606,208.00	400,782,112.00
2:V__ESCO.hru	Soil evaporation compensation factor	68,232,990,720.00	−24,410,099,712.00	222,638,145,536.00
3:V__CH_K2.rte	Effective hydraulic conductivity in tributary channel alluvium	1,349,529,216.00	−452,413,600.00	1,358,584,192.00
4:R__SOL_AWC.sol	Available water capacity of the soil layer	−561,091,456.00	−41,671,454,720.00	7,562,514,432.00
5:R__SOL_BD.sol	Moist bulk density	−698,324,288.00	−1,564,002,560.00	426,062,400.00
6:A__GWQMN.gw	Threshold depth of water in the shallow aquifer required for return flow to occur	−68,436,328.00	−148,884,752.00	154,694,208.00
7:V__REVAPMN.gw	Threshold depth of water in the shallow aquifer required for revap or percolation to the deep aquifer to occur	−17,208,166.00	−19,586,908.00	23,662,928.00
8:R__SLSUBBSN.hru	Average slope length	−17,792,028.00	−23,848,322.00	8,888,399.00
9:R__SFTMP.bsn	Snow melt base temperature	−3,711,943.00	−11,639,615.00	1,044,660.38
10:R__SMTMP.bsn	Snow melt base temperature	16,009.14	−16,503.95	16,504.26
11:V__ALPHA_BNK.rte	Base flow alpha factor	0.89	−0.03	1.52
12:R__SOL_K.sol	Saturated hydraulic conductivity	−0.06	−0.28	0.04
13:R__CN2.mgt	Initial SCS runoff curve number for moisture condition	−0.13	−0.36	0.01
14:V__SFTMP.bsn	Snowfall temperature	4.15	−5.00	5.00

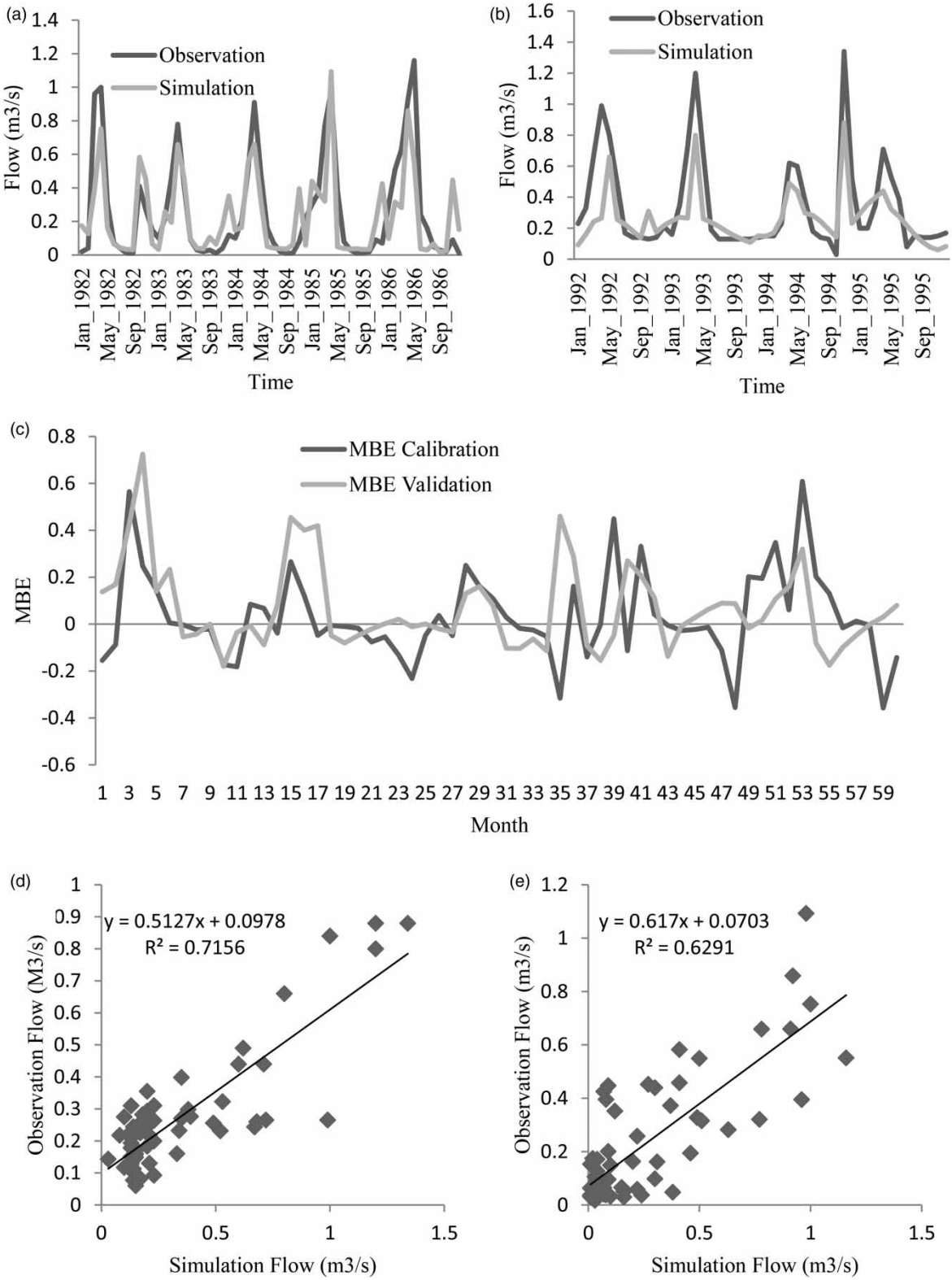

Figure 4 | (a) Comparison of monthly mean in the calibration period, (b) comparison of monthly average in the validation period, (c) MBE in the calibration and validation period, (d) correlation coefficient in the calibration period, and (e) correlation coefficient in the validation period.

and March (30 mm). By examining Figure 3(b), the highest model error at maximum temperature and minimum temperature in Mehr Abad was 2.3 °C in November and 2.3 °C decrease in September. At the Northern Tehran station, the highest model error at maximum and minimum temperatures was 2.5 °C decrease in September and 1.4 °C increase in August.

Following a trial and error approach for selecting the effective parameters (Table 3), a total of 14 parameters affecting the precipitation-runoff simulation using the SWAT-CUP model were identified. Investigating the results of *t*-stat and *p*-value in Table 5, it was found that the SMTMP and SFTMP were the most significant parameters affecting the analysis of the uncertainty. The study area was a small watershed where precipitations in the form of snow are common during the winter time, especially January and February. This snow then serves as a source for the runoffs developed during March and April. This led us toward selecting the above-mentioned two parameters that largely contribute to the melting of the snow. Investigating the uncertainty of the SWAT-CUP model (Figure 4), it was observed that the SWAT model was rendered uncertain when simulating the precipitation-runoff data at peak values. Much of this uncertainty had occurred during spring season, especially during March and April. As indicated in Table 5, the runoffs developed during the March and April were consequences of the precipitation occurring in the form of snow across the study area during January and February; the SWAT model failed to consider this cause of the runoffs in the respective simulations.

Based on Table 4, it can be stipulated that fairly good results were obtained during the calibration and evaluation periods across the study area. Moreover, the value of P-factor was found to be larger than 0.5, indicating the appropriate performance of the model in simulating the precipitation-runoff data. By examining the form (Figure 4(a)) in the calibration period, as can be seen, the model has a proper function and it can be said that only in the maximum and minimum values, it has made errors and, as can be seen in Figure 4(b), the model performed appropriately in the validation period and it has made errors in only simulating limiting values. In general, by examining the mean square error (MBE) in Figure 4(c), as seen, the maximum model error in the calibration period is 0.6 and in the validation period it is 0.72, which indicates the proper performance of the model. The correlation coefficient for the calibration period is generally 0.63 and for the validation period it is generally 0.71 (Figure 4(d) and 4(e)).

Table 4 | Examining error and uncertainty parameters in calibration and validation periods

Variable	P-factor	R-factor	R^2	NS
Calibration	0.58	0.68	0.63	0.62
Validation	0.55	0.58	0.71	0.69

Based on the studies performed by Jimeno-Sáez *et al.* (2018), the results are not satisfactory, satisfactory, fairly good, and very good if the value of the NSE is smaller than 0.3, ranges between 0.3 and 0.5, ranges between 0.5 and 0.7, and exceeds 0.7, respectively. Based on Table 4, it can be stipulated that fairly good results were obtained during the calibration and evaluation periods across the study area. Moreover, the value of P-factor was found to be larger than 0.5, indicating appropriate performance of the model in simulating the precipitation-runoff data.

Precipitation and temperature modeling in upcoming period

The minimum and maximum precipitation and temperature were simulated using the SDSM under three RCP (2.6, 4.5, and 8.5) scenarios for the upscaled CanESM2 model in the three periods, 2010–2040, 2041–2070, and 2071–2100, and the results are presented in Figure 5 and Table 5.

In addition, Figure 5 shows the simulation for each station in the assessment period (historical data of the CanESM2 model during 1961–2005).

According to Table 5 and Figure 5 regarding the precipitation at Roodbar Ghasran station in all seasons, except for summer, the increased precipitation is observed in all periods. This is also the case in Roodak and Fasham stations, and there is an increasing trend in all seasons. However, it should be noted that during the period 2041–2100 in the Fasham station, the precipitation decrease is observed during spring.

The changes are different at Mehr Abad and Northern Tehran stations. The only similarity with the other three stations is in the process of decreased precipitation in the

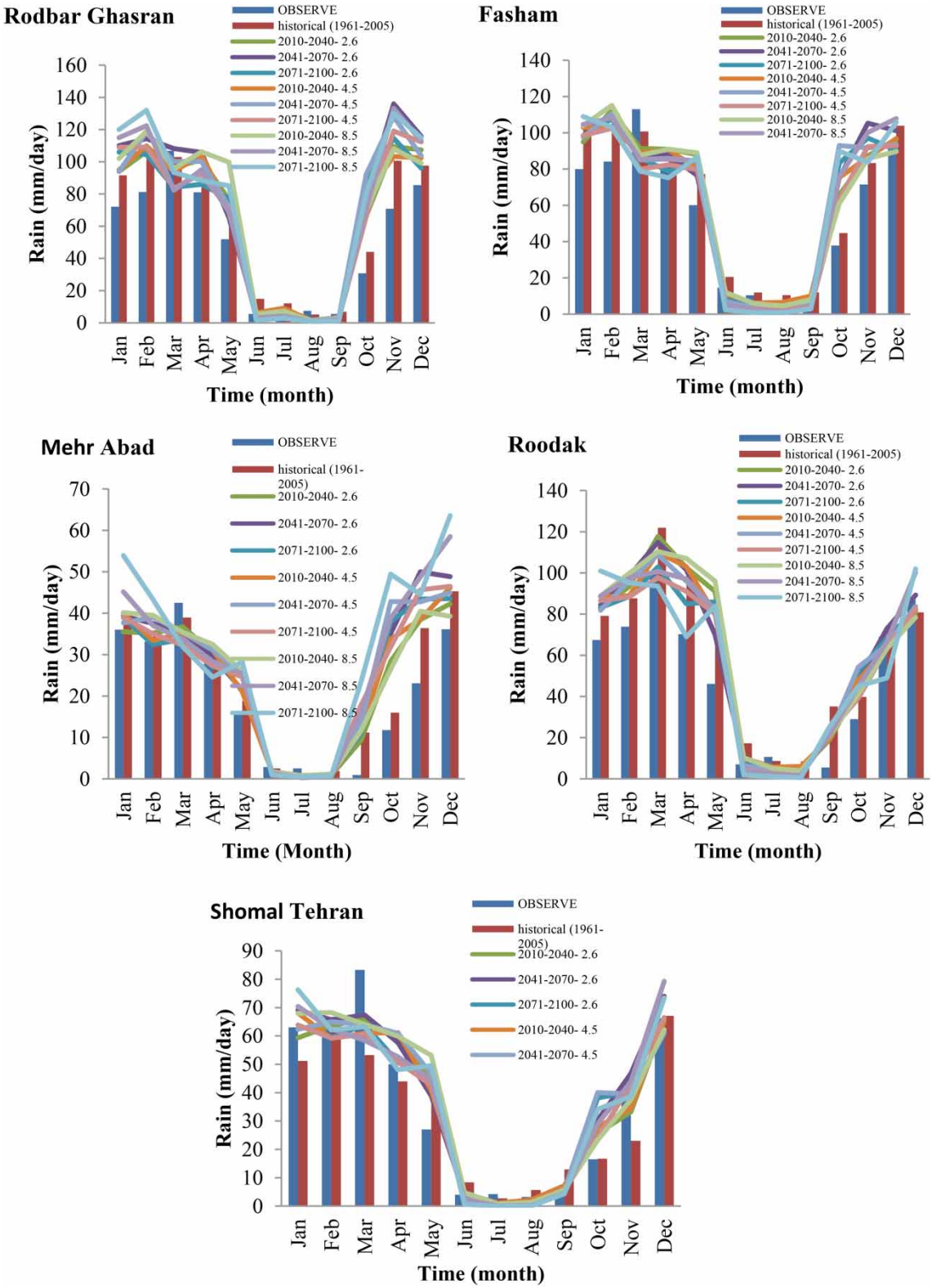

Figure 5 | Variations in precipitation during the historical period and three subsequent periods under three scenarios.

Table 5 | Variations in precipitation under three different scenarios during three different periods

Station name	Scenario Season	2.6 Winter	Spring	Summer	Fall	4.5 Winter	Spring	Summer	Fall	8.5 Winter	Spring	Summer	Fall
Fasham	2010–2040	−15.22	−4.76	3.22	−15.13	−14.92	−1.29	2.45	−18.74	−17.01	−3.82	2.92	−13.05
Fasham	2041–2070	−18.28	1.42	4.44	−23.57	−14.66	0.38	5.81	−25.00	−21.01	0.07	7.40	−21.07
Fasham	2071–2100	−12.92	2.57	4.56	−23.56	−12.04	4.70	7.24	−14.67	−20.06	5.12	9.07	−20.35
Roodbar Ghasran	2010–2040	−22.95	−11.44	1.93	−23.77	−22.80	−9.89	1.66	−26.44	−27.08	−20.60	2.63	−24.69
Roodbar Ghasran	2041–2070	−33.78	−13.25	2.58	−36.67	−25.77	−10.85	3.04	−38.68	−37.16	−2.10	4.51	−32.86
Roodbar Ghasran	2071–2100	−22.59	−2.57	2.83	−32.85	−30.54	−2.10	3.77	−26.87	−42.69	−9.04	5.45	−34.87
Roodak	2010–2040	−9.47	−31.87	2.05	−9.12	−10.27	−25.74	0.85	−9.24	−12.86	−32.57	1.72	−7.34
Roodak	2041–2070	−14.62	−23.58	2.51	−13.12	−11.17	−23.39	3.59	−12.36	−19.36	−21.34	5.49	−9.84
Roodak	2071–2100	−8.58	−19.40	3.16	−12.30	−9.79	−17.70	5.01	−7.33	−23.25	−10.29	6.98	−5.29
Mehr Abad	2010–2040	−2.56	−1.34	1.15	−13.44	−4.71	0.21	1.09	−16.00	−4.53	−1.92	1.04	−14.28
Mehr Abad	2041–2070	−6.78	0.64	1.11	−21.18	−5.44	−1.29	1.22	−20.97	−11.79	0.15	1.50	−22.59
Mehr Abad	2071–2100	−3.20	0.80	1.16	−18.84	−5.05	1.28	1.33	−19.85	−18.50	1.12	1.52	−27.20
Shomal Tehran	2010–2040	2.44	−3.35	1.60	−0.89	1.15	−0.87	1.23	−2.80	−0.89	−5.59	1.54	−1.74
Shomal Tehran	2041–2070	−4.37	−1.18	2.00	−7.34	2.39	−3.76	2.48	−8.03	−5.51	1.60	2.93	−5.40
Shomal Tehran	2071–2100	3.92	0.43	2.16	−7.79	2.05	2.07	2.90	−3.97	−5.35	−0.16	3.60	−5.30

summer and the rise in the fall, and it shows different behaviors in spring and winter, as shown in Table 5. Most changes are observed in all periods in the fall and winter seasons, and the variations in each three periods and each scenario can be seen in Figure 4 and Table 5. The precipitation variation is different in the periods, but in most stations in all four seasons, the changes mostly occur during the period 2041–2070.

All units are expressed in mm and show the difference between the average observational period and the estimated period by the model. The negative values indicate an increase and the positive values indicate a decrease in the precipitation.

Reviewing the maximum temperature and minimum temperature in Figure 6 and Table 6 shows that the highest increasing trend of temperature occurs in the winter and summer temperatures. In all periods, the highest temperature rise is during the period 2071–2100. The changes in all seasons for all the periods and all the scenarios can be seen in Table 6.

Runoff modeling in the upcoming period

To simulate the runoff in the upcoming period, after selecting the effective parameters for the runoff simulation in the SWAT_CUP model and entering the SWAT model, the

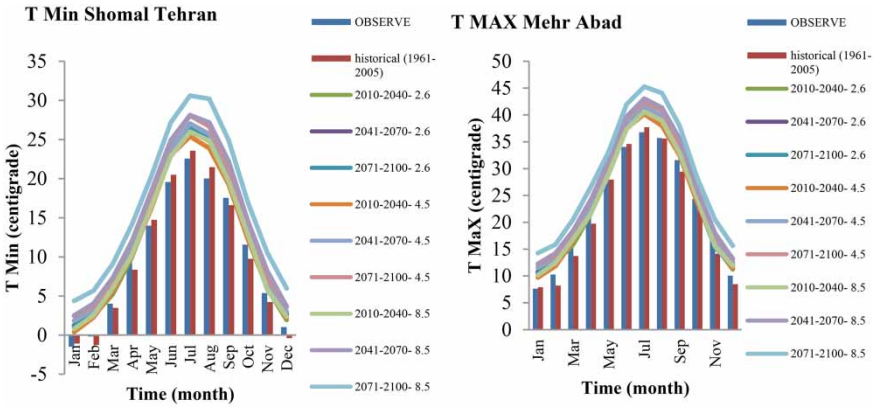

Figure 6 | Variations in the historical period and three subsequent periods under three scenarios.

Table 6 | Temperature variations under three different scenarios in three different periods

Station name	Scenario / Season	2.6 Winter	Spring	Summer	Fall	4.5 Winter	Spring	Summer	Fall	8.5 Winter	Spring	Summer	Fall
T max Mer Abad	2010–2040	−2.09	−0.61	−3.53	−0.11	−1.72	−0.82	−3.03	0.17	−2.19	−0.70	−3.45	−0.12
T max Mer Abad	2041–2070	−2.43	−1.47	−3.92	−0.53	−3.15	−2.03	−4.46	−0.99	−3.89	−2.96	−5.85	−2.36
T max Mer Abad	2071–2100	−2.43	−2.00	−3.89	0.01	−3.77	−2.78	−5.39	−1.59	−5.94	−5.01	−8.25	−4.73
T min Mer Abad	2010–2040	−0.72	−0.36	−3.30	0.39	−0.43	−0.52	−2.85	0.61	−0.83	−0.41	−3.23	0.39
T min Mer Abad	2041–2070	−1.06	−1.12	−3.65	−0.02	−1.62	−1.58	−4.13	−0.40	−2.31	−2.41	−5.38	−1.66
T min Mer Abad	2071–2100	−1.05	−1.55	−3.62	0.44	−2.19	−2.26	−5.02	−0.97	−4.10	−4.22	−7.65	−3.79
T max Shomal Tehran	2010–2040	−2.33	−0.65	−4.22	−0.65	−2.08	−0.83	−3.66	−0.41	−2.47	−0.96	−4.13	−0.66
T max Shomal Tehran	2041–2070	−2.79	−1.68	−4.68	−1.19	−3.45	−2.17	−5.26	−1.71	−4.35	−3.15	−6.78	−3.29
T max Shomal Tehran	2071–2100	−2.74	−2.06	−4.73	−0.68	−4.13	−2.90	−6.42	−2.30	−6.62	−5.48	−9.75	−6.05
T min Shomal Tehran	2010–2040	−2.01	−1.33	−3.95	−1.24	−1.83	−1.45	−3.37	−1.02	−2.11	−1.68	−3.84	−1.30
T min Shomal Tehran	2041–2070	−2.38	−2.20	−4.34	−1.79	−2.88	−2.61	−4.79	−2.22	−3.62	−3.34	−6.01	−3.50
T min Shomal Tehran	2071–2100	−2.29	−2.41	−4.37	−1.33	−3.47	−3.13	−5.78	−2.61	−5.55	−5.28	−8.61	−5.97

runoff was simulated for the period 2010–2040 using the SWAT model for the upcoming period. Figure 7 shows the variations of runoff in three scenarios over the period 2010–2040. As can be seen, the changes are mostly observed in March and May, and there is an increasing trend of more than 0.5 m^3/s, respectively. And the lowest changes occurred in August. Table 7 generally shows the variations in full. By reviewing the annual results, the increasing changes are very low at 0.1 m^3/s, and the increasing trend in the RCP 8.5 scenario is higher than other scenarios (0.16 m^3/s). By reviewing the results in the seasons, the highest changes occur in the spring and the lowest in the summer and the characteristics of the variations can be seen in Table 7. In general, it can be stated that there is an increase in precipitation in the spring and summer and there is a decrease in the runoff in summer.

DISCUSSION

In general, the goals were accomplished in this study. The purpose of this study was to investigate the performance of SDSM and CanESM2 model, evaluate the performance of the SWAT model in the precipitation and runoff simulation, and finally, to study the climate change process and its effect on runoff. In the next section, the questions asked in the introduction are answered, respectively.

In general, the changes were considered regarding the precipitation, maximum temperature, and minimum temperature in the period 2010–2100, which was divided into three periods, and the changes were reviewed in relation to runoff during the period 2010–2040. In general, the effect of climate change on runoff was evaluated under three scenarios.

The performance of the SDSM was evaluated as suitable in the Canems2 model downscaling, and the results are shown in Figure 3. The results obtained in this study are similar to those of other studies (Pradhan-Salike & Pokharel 2017; Iwadra *et al.* 2018).

The performances of the SWAT and SWAT-CUP models were evaluated as satisfactorily, so that the ENS was obtained in the calibration and evaluation period equal to 0.71 and 0.6, respectively. The results related to the runoff simulation are similar to the studies like Saha *et al.* (2014) and Dhami *et al.* (2018).

As discussed in the Results section, the highest changes were observed in the fall and winter, with the lowest changes observed in summer. It is also necessary to note that the Mehr Abad and Northern Tehran stations are located in the plains and lowlands, while the other stations are located at highlands and in mountainous areas. All the stations show an increasing trend during the upcoming periods. According to Table 9, the highest changes were observed in Mehrabad station and the lowest changes were observed in the Northern Tehran station. The variations in the stations are different, but in most stations, the highest increasing changes occurred in all three scenarios during the period 2040–2070. The highest increase in precipitation in the RCP 8.5 scenario was observed at Mehrabad station with a 52% increase and the lowest

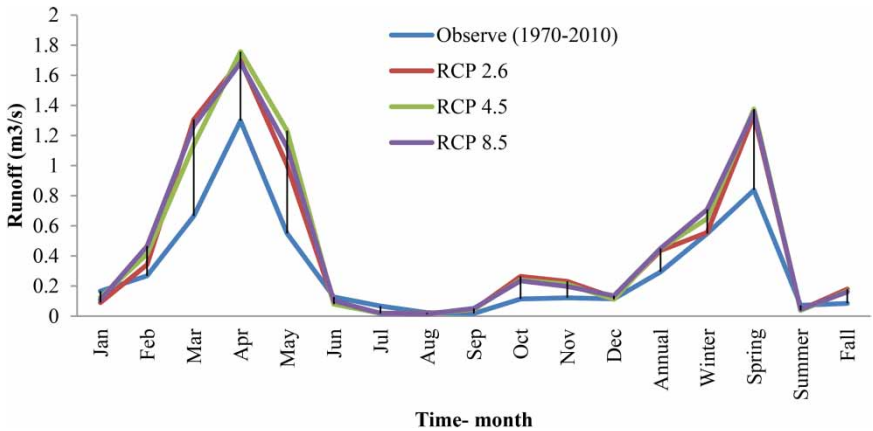

Figure 7 | Variations in monthly, seasonal, and annual runoff during period 2010–2040 under three scenarios.

Table 7 | Seasonal, monthly, and annual runoff variations over period 2010–2040 under three scenarios

	Jan	Feb	Mar	Apr	May	Jun	Jul	Aug	Sep	Oct	Nov	Dec	Annual	Winter	Spring	Summer	Fall
Change 2.6	0.08	−0.07	−0.64	−0.40	−0.45	0.04	0.05	0.00	−0.03	−0.15	−0.11	−0.01	−0.14	−0.01	−0.50	0.03	−0.09
Change 4.5	0.04	−0.14	−0.47	−0.46	−0.68	0.05	0.05	0.01	−0.03	−0.13	−0.09	0.00	−0.15	−0.10	−0.54	0.03	−0.08
Change 8.5	0.06	−0.20	−0.60	−0.39	−0.57	0.03	0.05	0.01	−0.03	−0.12	−0.08	−0.02	−0.16	−0.16	−0.52	0.03	−0.08

Note: All units are in m^3/s, the negative values indicate runoff increase, and the positive values indicate the runoff decrease.

increase in Northern Tehran station in RCP 2.6 and 4.5 scenarios. In general, in the areas upstream of the study area, which includes the Fashem, Roodbar Ghasran, and Roodak stations, an increase in precipitation is observed between 6 and 39%, while in the downstream areas, there is an increase of 1–52%. Table 8 generally shows the variations in each of the three scenarios in each three stations during three different periods.

By examining the maximum temperature and minimum temperature in the results, the temperature rise is observed in all seasons. The highest changes were observed in the fall and winter. The least variations were observed in the period 2010–2040 and the highest variations were observed in the period 2071–2100. The variation in the RCP 8.5 scenario is higher than other scenarios, which are similar to the results of other studies. In general, it can be stated that in the period 2010–2100, the maximum temperature will vary from 1 to 6 °C, and the detailed specifications can be seen in Table 9.

By reviewing the runoff variations in the upcoming period (2010–2040) under the three RCP 2.6, RCP 4.5, and RCP 8.5 scenarios, an increasing trend is found equal to 0.14, 0.15, and 0.16 in the runoff of the upcoming period, respectively, so that the highest changes in all three scenarios were observed in the spring. In fact, it can be stated that in the spring, winter, and summer, the increase in runoff was observed, and in the fall, there was a decrease in the runoff. In general, it can be stated that in the period 2010–2040 in three RCP 2.6, RCP 4.5, and RCP 8.5

Table 8 | Variations in precipitation in three scenarios during three different periods

	Fasham	Roodbar Ghasran	Roodak	Mehrabad	Shomal tehran
CH 2010–2040 2.6	14.61	26.85	24.52	18.52	0.60
CH 2041–2070 2.6	16.47	39.06	24.74	31.03	6.82
CH 2071–2100 2.6	13.45	26.34	18.64	23.37	0.15
CH 2010–2040 4.5	14.88	27.46	22.44	22.55	0.15
CH 2041–2070 4.5	15.33	34.72	21.88	31.40	4.07
CH 2071–2100 4.5	6.83	26.62	14.83	26.15	2.85
CH 2010–2040 8.5	14.18	33.48	25.90	22.89	3.91
CH 2041–2070 8.5	15.84	32.43	22.78	39.20	3.69
CH 2071–2100 8.5	12.03	39.08	15.90	52.10	4.27

Note: All units are in %, and CH stands for Change.

Table 9 | Temperature variations in three scenarios over three different periods

		2.6	4.5	8.5
T max Mer Abad	2010–2040	1.59	1.35	1.62
T max Mer Abad	2041–2070	2.09	2.66	3.77
T max Mer Abad	2071–2100	2.08	3.38	5.98
T min Mer Abad	2010–2040	1.00	0.80	1.02
T min Mer Abad	2041–2070	1.46	1.93	2.94
T min Mer Abad	2071–2100	1.44	2.61	4.94
T max Shomal Tehran	2010–2040	1.97	1.75	2.06
T max Shomal Tehran	2041–2070	2.59	3.15	4.40
T max Shomal Tehran	2071–2100	2.56	3.95	6.98
T min Shomal Tehran	2010–2040	2.14	1.92	2.24
T min Shomal Tehran	2041–2070	2.68	3.13	4.13
T min Shomal Tehran	2071–2100	2.61	3.76	6.36

scenarios, the runoff is increased by 45, 49, and 50%, respectively.

The results obtained in this study are similar to those of other studies performed in Iran (Samadi *et al.* 2013; Sarzaeim *et al.* 2017; Mirdashtvan *et al.* 2018).

CONCLUSION

It should be noted that the Darabad study area is located upstream of the big Tehran watershed in a mountainous area. This region has snowfall at heights during winter. The results of this study showed that the minimum temperature and maximum temperature are increased in winter, as well as the amount of precipitation. It should be noted that the runoff in the fall is dependent on the snowfall runoff in winter. When the temperature and precipitation are increased in these seasons, it causes the snow on the mountain to be melted earlier and eventually cause more runoff in the spring, which ultimately causes flooding. It can be stated that in the past, even at the end of spring, there was snow on the peaks of Tehran. The heavy rains have also increased in the spring, especially comparing the seasonal statistics for the previous years, as the precipitation has been reduced in the spring and its amount and intensity have been increased, causing flash floods. All these factors indicate climate change and its impact on the floods and droughts, which is very important in long-term planning, especially for the metropolitan areas such as Tehran. It should be reminded that the floods with different return periods pose serious financial and life risks to the upstream of Tehran. It is suggested that future research should focus on sediment, soil erosion, and other empirical models to simulate the runoff.

Moreover, the floods that occurred in spring 2019, especially in May in Lorestan, Kermanshah, Golestan, and Tehran provinces, show that the models have worked correctly in the simulation, and the climate change model and the fifth-generation scenario have exhibited good performance in the climate change estimates.

REFERENCES

Abbaspour, K. C., Rouholahnejad, E., Vaghefi, S., Srinivasan, R., Yang, H. & Kløve, B. 2015 A continental-scale hydrology and water quality model for Europe: calibration and uncertainty of a high-resolution large-scale SWAT model. *Journal of Hydrology* **524**, 733–752.

Ahmadi, M., Ahmadi, H., Moeini, A. & Zehtabiyan, G. R. 2019a Assessment of climate change impact on surface runoff, statistical downscaling and hydrological modeling. *Physics and Chemistry of the Earth, Parts A/B/C* **114**, 102800.

Ahmadi, M., Moeini, A., Ahmadi, H., Motamedvaziri, B. & Zehtabiyan, G. R. 2019b Comparison of the performance of SWAT, IHACRES and artificial neural networks models in rainfall-runoff simulation (case study: Kan watershed, Iran). *Physics and Chemistry of the Earth, Parts A/B/C* **111**, 65–77.

Al-mukhtar, M. 2016 Modelling the root zone soil moisture using artificial neural networks, a case study. *Environmental Earth Sciences* **75** (15), 1124.

Arnold, J. G., Moriasi, D. N., Philip, W., Abbaspour, K. C. & White, M. J. 2012 SWAT: model use, calibration, and validation. *Transactions of the ASABE* **55** (4), 1549–1559. http://elibrary.asabe.org/abstract.asp??JID=3&AID=42263&CID=t2012&v=55&i=4&T=1.

Ashraf Vaghefi, S., Mousavi, S. J., Abbaspour, K. C., Srinivasan, R. & Yang, H. 2014 Analyses of the impact of climate change on water resources components, drought and wheat yield in semiarid regions: Karkheh River Basin in Iran. *Hydrological Processes* **28** (4), 2018–2032.

Awan, U. K., Liaqat, U. W., Choi, M. & Ismaeel, A. 2016 A SWAT modeling approach to assess the impact of climate change on consumptive water use in Lower Chenab Canal area of Indus basin. *Hydrology Research* **47** (5), 1025–1037.

da Silva, R. M., Dantas, J. C., de Araújo Beltrão, J. & Santos, C. A. G. 2018 Hydrological simulation in a tropical humid

basin in the Cerrado biome using the SWAT model. *Hydrology Research* **49** (3), 908–923.

Dehghan, Z., Fathian, F. & Eslamian, S. 2019 Climate change impact on agriculture and irrigation network. In: *Climate Change-Resilient Agriculture and Agroforestry*. (P. Castro, A. M. Azul, W. L. Filho & U. M. Azeiteiro, eds.) Springer, Cham, Switzerland, pp. 333–354.

Deng, Z., Zhang, X. & Li, D. 2014 Simulation of Land Use/Land Cover Change and Its Effects on the Hydrological Characteristics of the Upper Reaches of the Hanjiang Basin.

Dhami, B., Himanshu, S. K., Pandey, A. & Gautam, A. K. 2018 Evaluation of the SWAT model for water balance study of a mountainous snowfed river basin of Nepal. *Environmental Earth Sciences* **77** (1), 21.

Dinpashoh, Y., Singh, V. P., Biazar, S. M. & Kavehkar, S. 2019 Impact of climate change on streamflow timing (case study: Guilan Province). *Theoretical and Applied Climatology* **138** (1–2), 65–76.

Gagnon, S., Singh, B., Rousselle, J. & Roy, L. 2005 An application of the statistical downscaling model (SDSM) to simulate climatic data for streamflow modelling in Québec. *Canadian Water Resources Journal* **30** (4), 297–314.

Gyamfi, C., Ndambuki, J. M. & Salim, R. W. 2016 Application of SWAT model to the Olifants Basin: calibration, validation and uncertainty analysis. *Journal of Water Resource and Protection* **8**, 397–410.

Hassan, Z., Shamsudin, S. & Harun, S. 2014 Application of SDSM and LARS-WG for simulating and downscaling of rainfall and temperature. *Theoretical and Applied Climatology* **116** (1–2), 243–257.

Houghton, J. T., Jenkins, G. J. & Ephraums, J. J. 1991 *Climate Change*.

Huo, A. & Li, H. 2013 Assessment of climate change impact on the stream-flow in a typical debris flow watershed of Jianzhuangcuan catchment in Shaanxi Province, China. *Environmental Earth Sciences* **69**, 1931–1938.

Iwadra, M., Odirile, P. T., Parida, B. P. & Moalafhi, D. B. 2018 Evaluation of future climate using SDSM and secondary data (TRMM and NCEP) for poorly gauged catchments of Uganda: the case of Aswa catchment. *Theoretical and Applied Climatology* **137** (3–4), 2029–2048.

Jaiswal, R. K., Tiwari, H. L. & Lohani, A. K. 2017 Assessment of climate change impact on rainfall for studying water availability in upper Mahanadi catchment, India. *Journal of Water and Climate Change* **8** (4), 755–770.

Jimeno-Sáez, P., Senent-Aparicio, J., Pérez-Sánchez, J. & Pulido-Velazquez, D. 2018 A comparison of SWAT and ANN models for daily runoff simulation in different climatic zones of peninsular Spain. *Water* **10** (2), 192.

Klein, N. 2015 *This Changes Everything: Capitalism vs. the Climate*. Simon and Schuster, New York, USA.

Mirdashtvan, M., Najafinejad, A., Malekian, A. & Sa'doddin, A. 2018 Downscaling the contribution to uncertainty in climate-change assessments: representative concentration pathway (RCP) scenarios for the South Alborz Range, Iran. *Meteorological Applications* **25** (3), 414–422.

Narsimlu, B., Gosain, A. K. & Chahar, B. R. 2013 Assessment of future climate change impacts on water resources of Upper Sind River Basin, India using SWAT model. *Water Resources Management* **27** (10), 3647–3662.

Nazari-Sharabian, M., Karakouzian, M. & Ahmad, S. 2019 Watershed-Scale Surface Runoff and Water Quality Response to Climate Change, Urbanization, and Implementation of LIDs.

Noori, N. & Kalin, L. 2016 Coupling SWAT and ANN models for enhanced daily streamflow prediction. *Journal of Hydrology* **533**, 141–151. http://doi.org/10.1016/j.jhydrol.2015.11.050.

Park, J.-Y., Yu, Y.-S., Hwang, S.-J., Kim, C. & Kim, S.-J. 2014 SWAT modeling of best management practices for Chungju dam watershed in South Korea under future climate change scenarios. *Paddy and Water Environment* **12** (1), 65–75.

Pradhan-Salike, I. & Pokharel, J. R. 2017 Impact of urbanization and climate change on urban flooding: a case of the Kathmandu valley. *Journal of Natural Resources and Development* **7**, 56–66.

Rahimi, J., Malekian, A. & Khalili, A. 2018 Climate change impacts in Iran: assessing our current knowledge. *Theoretical and Applied Climatology* **135** (1–2), 545–564.

Raziei, T., Arasteh, P. D. & Saghfian, B. (2005) Annual rainfall trend in arid and semi-arid regions of Iran. *ICID 21st European Regional Conference*, May, pp. 1–8.

Rostamian, R., Jaleh, A., Afyuni, M., Mousavi, S. F., Heidarpour, M., Jalalian, A. & Abbaspour, K. C. 2008 Application of a SWAT model for estimating runoff and sediment in two mountainous basins in central Iran. *Hydrological Sciences Journal* **53** (5), 977–988.

Saha, P. P., Zeleke, K. & Hafeez, M. 2014 Streamflow modeling in a fluctuant climate using SWAT: Yass River catchment in south eastern Australia. *Environmental Earth Sciences* **71** (12), 5241–5254.

Samadi, S., Carbone, G. J., Mahdavi, M., Sharifi, F. & Bihamta, M. R. 2013 Statistical downscaling of river runoff in a semi arid catchment. *Water Resources Management* **27** (1), 117–136.

Sanz-Perez, E. S., Murdock, C. R., Didas, S. A. & Jones, C. W. 2016 Direct capture of CO_2 from ambient air. *Chemical Reviews* **116** (19), 11840–11876.

Sarzaeim, P., Elahe, O. B. & Loa, H. A. 2017 Climate Change Outlook for Water Resources Management in a Semiarid River Basin: The Effect of the Environmental Water Demand.

Shahvari, N., Khalilian, S., Mosavi, S. H. & Mortazavi, S. A. 2019 Assessing climate change impacts on water resources and crop yield: a case study of Varamin plain basin, Iran. *Environmental Monitoring and Assessment* **191** (3), 134.

Tavakol-Davani, H., Nasseri, M. & Zahraie, B. 2013 Improved statistical downscaling of daily precipitation using SDSM platform and data-mining methods. *International journal of climatology* **33** (11), 2561–2578.

Vera, C., Silvestri, G., Liebmann, B. & González, P. 2006 Climate change scenarios for seasonal precipitation in South America from IPCC-AR4 models. *Geophysical Research Letters* **33** (13).

Wilby, R. L. & Dawson, C. W. (2007) SDSM 4.2 – A Decision Support Tool for the Assessment of Regional Climate Change Impacts. United Kingdom.

Wilby, R. L., Dawson, C. W. & Barrow, E. M. 2002 SDSM – a decision support tool for the assessment of regional climate change impacts. *Environmental Modelling & Software* **17** (2), 145–157.

Worqlul, A. W., Ayana, E. K., Yen, H., Jeong, J., MacAlister, C., Taylor, R., Gerik, T. J. & Steenhuis, T. S. 2018 Evaluating hydrologic responses to soil characteristics using SWAT model in a paired-watersheds in the Upper Blue Nile Basin. *Catena* **163**, 332–341.

Zehtabian, G. R., Salajegheh, A., Malekian, A., Boroomand, N. & Azareh, A. 2016 Evaluation and comparison of performance of SDSM and CLIMGEN models in simulation of climatic variables in Qazvin plain. *Desert* **21** (2), 155–164.

First received 4 May 2019; accepted in revised form 25 November 2019. Available online 9 December 2020